Spontaneous toroidal rotation driven by the off-diagonal term of momentum and heat transport in the plasma with the ion internal transport barrier in LHD

To cite this article: K. Ida *et al* 2010 *Nucl. Fusion* **50** 064007

IOP Publishing and International Atomic Energy Agency Nuclear Fusion
Nucl. Fusion **50** (2010) 064007 (8pp) doi:10.1088/0029-5515/50/6/064007

Spontaneous toroidal rotation driven by the off-diagonal term of momentum and heat transport in the plasma with the ion internal transport barrier in LHD

K. Ida[1], M. Yoshinuma[1], K. Nagaoka[1], M. Osakabe[1], S. Morita[1], M. Goto[1], M. Yokoyama[1], H. Funaba[1], S. Murakami[2], K. Ikeda[1], H. Nakano[1], K. Tsumori[1], Y. Takeiri[1], O. Kaneko[1] and LHD experiment group

[1] National Institute for Fusion Science, Toki, Gifu 509-5292, Japan
[2] Department of Nuclear Engineering, Kyoto University, Kyoto, 606-8501, Japan

Received 17 October 2009, accepted for publication 6 May 2010
Published 28 May 2010
Online at stacks.iop.org/NF/50/064007

Abstract
A spontaneous rotation in the co-direction is observed in plasmas with an ion internal transport barrier (ITB), where the ion temperature gradient is relatively large ($\partial T_i/\partial r \sim 5\,\mathrm{keV\,m^{-1}}$ and $R/L_{T_i} \sim 10$) in LHD. Because of the large ion temperature gradients, the magnitude of the spontaneous toroidal flow, V_ϕ^{spon}, becomes large enough to cancel the toroidal flows driven by tangential injected neutral beams and the net toroidal rotation velocity is almost zero at the outer half of the plasma minor radius even in the plasmas with counter-dominant NB injections. The effect of velocity pinch is excluded even if it exits because of zero rotation velocity. The spontaneous toroidal flow appears in the direction of co-rotation after the formation of the ITB, not during or before the ITB formation. The causality between the change in V_ϕ^{spon} and $\partial T_i/\partial r$ observed in this experiment clearly shows that the spontaneous rotation is driven by the ion temperature gradient as the off-diagonal terms of momentum and heat transport.

PACS numbers: 52.55.Hc, 52.55.Fa, 52.50.Sw, 52.50.Gj

(Some figures in this article are in colour only in the electronic version)

1. Introduction

Spontaneous rotation has been observed in many tokamaks. It has been observed in ohmic discharges in PLT [1], PDX [2] and Alcator C-mod [3], where there is no external momentum input. The spontaneous rotation becomes more significant in the plasmas with additional heating with no-momentum input such as ICRF heating in JIPP-TIIU [4], JET [5], Alcator C-mode [6] and ECH in CHS [7] and D-IIID [8]. The rotation can be either in the same (co) or opposite (counter) directions as the plasma current; the rotation is usually co in H-mode and counter in the internal transport barrier (ITB)-mode and can be either co or counter in L-mode depending on the plasma conditions. The momentum transport analysis to investigate the mechanism of spontaneous rotation has been done, and a non-diffusive term of the momentum transport was found in JT-60U [9] and JFT-2M [10]. These experiments suggest that the spontaneous rotation is peaked at the plasma centre and the radial profiles of spontaneous rotation are somewhat similar to that of ion temperature profiles. In contrast, the spontaneous rotation observed in plasmas with an ion ITB is peaked off-centre of the plasmas near the ITB region where the ion temperature gradient is large. The spontaneous rotation in the ITB region that is in the direction counter to the plasma current has been observed in JT-60U [11, 12], TFTR [13] and Alcator C-mod [14]. The large spontaneous rotation in the region of the ITB suggests that the temperature gradient is responsible for driving the spontaneous rotation and the radial profile of the spontaneous rotation is similar to the radial profiles of the temperature gradient rather than the temperature itself. More recently, the flip of direction of the spontaneous rotation is observed in TCV [15], which suggests that the driving mechanism of spontaneous rotations is a non-linear process. The physics mechanism determining the direction and magnitude of the spontaneous toroidal flow driven by turbulence is a crucial topic in toroidal plasmas. Because the

turbulence in plasmas is driven by temperature (or pressure) gradients, the spontaneous rotation is observed as the off-diagonal terms of momentum and heat transport [10]. The direction of the spontaneous toroidal flow varies depending on the plasmas; for example, it is in the co-direction (parallel to the plasma current) in the JET and Alcator C-Mod [6] plasmas while it is in the counter-direction (anti-parallel to the plasma current) in JFT-2M [10, 16] and JT-60U [12, 17] plasmas. The spontaneous rotation has been observed in the helical plasmas in CHS [7] and LHD [18], which suggests that the spontaneous rotation is a common feature in the momentum transport in the toroidal plasmas.

The mechanism of spontaneous rotation has been investigated theoretically. The profile shearing [19] and up–down asymmetry of the plasma flux surface [20]can provide an 'internal torque' potentially leading to spontaneous rotation. Also, the effect of the radial electric field shear on turbulent momentum transport has also been investigated [21]. The symmetry breaking of turbulence with the existence of radial electric field shear can produce an internal toroidal torque and results in the spontaneous velocity gradient [22]. The turbulence in the plasmas is driven by the temperature gradient and the radial electric field shear should be related to the curvature of the ion temperature profiles because $E_r \sim \partial T_i/\partial r$ when the pressure term is dominant in the radial force balance equation of bulk ions. Therefore, it is important to investigate the spontaneous toroidal rotation velocity gradient (not driven by the momentum flux due to the external torque), because the momentum flux due to the internal toroidal torque is directly related to the velocity gradient rather than the rotation velocity itself. The magnitude of the spontaneous rotation velocity is determined by the momentum transport equation with the boundary condition at the plasma periphery. For example, the plasma rotates in the counter-direction at the periphery due to the ripple loss of fast ion and the edge toroidal rotation velocity can be negative (in the counter-direction), when the ripple amplitude due to toroidal coils exceeds 1% in a tokamak [23].

In this paper, the relation between the velocity gradient driven by the internal torque and ion temperature gradient and curvature that are the candidates of the driving force of spontaneous rotations in the plasmas is described. Because spontaneous rotation is more significant in the plasmas with larger ion temperature gradients, the spontaneous rotation in the plasmas with the ITB [24] is discussed. In the discharge with carbon pellet injection, the density profile is peaked just after the pellet injection and it becomes flat as the electron density decreases afterwards. The spontaneous rotation appears associated with the increase in the ion temperature gradient (not the increase in the ion pressure gradient) during the decay phase of electron density. This observation suggests that the ion temperature gradient rather than the ion pressure gradient is the driving force of the spontaneous rotation velocity. The relations between the spontaneous rotation and the ion temperature gradient and the ion pressure gradient are also discussed.

2. Disparity of co- and counter-driven toroidal rotation profiles

Since spontaneous rotation due to the temperature gradient has the sign preference, either co- or counter-direction to the plasma current (equivalent toroidal current in helical plasmas), this spontaneous rotation appears as the disparity of co- and counter-driven toroidal rotation profiles in the discharges with co- and counter-neutral beam injection (NBI) with similar injection power. It should be noted that the velocity pinch due to the homogenization of toroidal angular momentum in different radii where the moment of inertia density varies due to the toroidal effect [25–27] does not cause the disparity of co- and counter-driven toroidal rotations. Figure 1 shows the radial profiles of toroidal rotation velocity, ion temperature and torque deposition in plasmas with one NBI (co- or counter-injection) and with three NBIs (2 co- 1 counter-injection and 1 co- 2 counter-injection) discharges in LHD. The sign of the toroidal rotation velocity is positive for co-rotation and negative for counter-rotation. In plasmas with one NBI the toroidal rotation profile in the plasmas with co-NBI is similar to the one in plasmas with counter-NBI except for the sign differences. Toroidal rotation velocity is measured from the Doppler shift of fully ionized carbon impurity with charge exchange spectroscopy [28] viewing the plasma tangentially. The main ion is hydrogen in this experiment. Since the measurements of toroidal rotation are done by carbon impurity, the velocity difference between the main ion and the impurity is evaluated with a neoclassical formula in the heliotron configuration [29]. The main ion rotates more in the co-direction than carbon impurities as seen in the dashed lines in figure 1. Therefore, the spontaneous rotation observed in the carbon impurity cannot be explained by the neoclassical effect. The spontaneous rotation evaluated for the main ions would be even larger than that evaluated by carbon impurity, because the spontaneous rotation observed in LHD is in the co-direction. In this plasma, the radial profiles of toroidal rotation velocity are determined mainly by the external torque due to the NBI and the radial diffusion of toroidal momentum and parallel viscosity which increases sharply towards the plasma edge which is similar to the toroidal rotation profiles reported in CHS [30, 31]. In heliotron plasmas no momentum pinch has been observed.

As seen in figures 1(e) and (f), the net toroidal torques are somewhat similar (especially between 1 ctr-NBI and 2ctr- plus 1co-NBIs) in the discharge with one counter-NBI and counter-dominant three NBIs. Here the deposited torque profiles are calculated using the FIT code based on the database calculated with a three-dimensional Monte Carlo simulation code [32] including orbit loss and charge exchange loss of fast ions. In plasmas with three NBIs, however, the radial profile of the toroidal rotation velocity in the plasmas with the counter-NBI dominant discharge is quite different from the one in the plasmas with the co-NBI dominant discharge. It should be noted that the plasma rotates in the co-direction at the half of the plasma minor radius in plasmas with the counter-NBI dominant discharge. The disparity of co- and counter-driven toroidal rotation profiles is significant in plasmas with three NBIs where the ion temperature gradient is large because of the formation of the ITB. Three NBIs are required to achieve the ITB plasmas in LHD. The sharp increase in toroidal rotation in the counter-direction near the plasma periphery is due to the spontaneous rotation driven by the positive radial electric field [7] which is strongly localized near the plasma edge in this discharge. The direction of the spontaneous rotation due

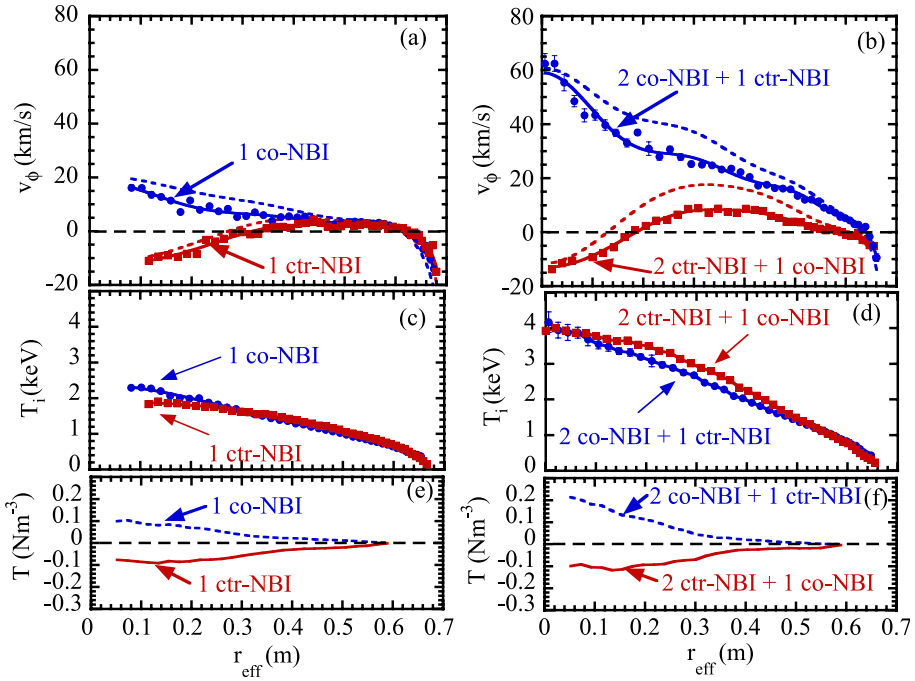

Figure 1. Radial profile of (*a*)(*b*) toroidal rotation velocity measured from carbon impurity (closed symbols), (*c*)(*d*) ion temperature and (*e*)(*f*) torque deposition for the plasma with (*a*)(*c*)(*e*) one NBI (co- and counter-injection) (*b*)(*d*)(*f*) three NBIs (2 co- 1 counter-injection and 1 co- 2 counter-injection) in LHD. The sign of the toroidal rotation velocity is positive for co-rotation and negative for counter-rotation). The dashed lines in (*a*) and (*b*) are toroidal rotation velocity profiles of main ions where the difference of rotation between the impurity and the main ion is evaluated with a neoclassical formula for the heliotron configuration.

to the radial electric field is opposite to the one observed in tokamak plasmas, where the spontaneous rotation in the co- (counter-) direction is observed in the region with positive (negative) electric fields [12].

Since the toroidal torque of co-NBI is similar to that of counter-NBI, the average of the toroidal rotation velocity in the plasmas with co-NBI and counter-NBI plotted in figure 2 (the sum of the two curves in figure 1(*a*) and (*b*) divided by 2) is considered to be the 'spontaneous toroidal rotation' due to the internal torque, which is also experimentally confirmed in the torque cancelling experiments in DIII-D [33]. The dashed lines in figure 2(*a*) are the toroidal rotation velocity profiles of the main ions where the difference in rotation between the impurity and the main ion is evaluated with a neoclassical formula for the heliotron configuration. Here, $r_{\rm eff}$ is the averaged minor radius on a magnetic flux surface and a_{99} is the effective minor radius in which 99% of the plasma kinetic energy is confined and is 0.64 m in this discharge. Although this averaged toroidal rotation is small in plasmas with L-mode (one NBI), it becomes significant in plasmas with an ITB (three NBIs) [24]. The ion temperature gradient at the effective minor radius, $r_{\rm eff}$, of 0.25 m in plasmas with three beams is 3–4 times larger than that in plasmas with one NBI. In the L-mode plasma, the temperature gradient increases in proportion to $\sqrt{P_{\rm NBI}}$ rather than $P_{\rm NBI}$. The spontaneous rotation evaluated by the average of the toroidal rotation velocity between co-NBI and counter-NBI is 15 km s^{-1} in the plasma core region, which is the same order of magnitude of the beam driven toroidal rotation velocity in LHD. The average of the toroidal rotation velocities of main ions (dashed lines) evaluated using a neoclassical formula for a heliotron configuration is larger than that evaluated for the carbon impurity and is 25 km s^{-1} for the ITB plasma with three beams and 5 km s^{-1} for the L-mode plasma with one beam. The sharp increase in the average toroidal rotation in the counter-direction at $r_{\rm eff} > a_{99}$ is driven by the large positive electric field due to the ergodic region outside the last closed surface, where the electrons escape along the magnetic field line while the ions are confined by helical ripples.

The radial profiles of the spontaneous toroidal rotation velocity evaluated by the balance between the neoclassical toroidal torque and the neoclassical parallel viscosity [30, 31] and the anomalous perpendicular viscosity ($\sim$4 m^2 s^{-1}) experimentally determined are plotted in figure 2(*c*). Here the radial electric field evaluated with the neoclassical theory is used. The spontaneous toroidal rotation of carbon impurity predicted by the neoclassical theory in the L-mode plasmas with one beam is in the counter-direction, which contradicts the observations because the carbon toroidal rotation measured is in the co-direction. In the ITB plasmas with three beams, the spontaneous toroidal rotation measured with carbon impurity is larger than that predicted with the neoclassical theory by a factor of two, which indicates the significant contribution of spontaneous rotation driven by turbulence. It is more important that the toroidal rotation velocity determined by the neoclassical theory does not have any bifurcation characteristics which causes the hysteresis of the spontaneous rotation described later in this paper (see figure 8), because it is determined mainly by the ion temperature gradient.

The time behaviour of the spontaneous toroidal rotation due to the ion temperature gradient should be different from the one driven by external torque, because it is the secondary effect of NBI associated with the increase in the ion temperature gradients. Therefore, it is expected that the spontaneous

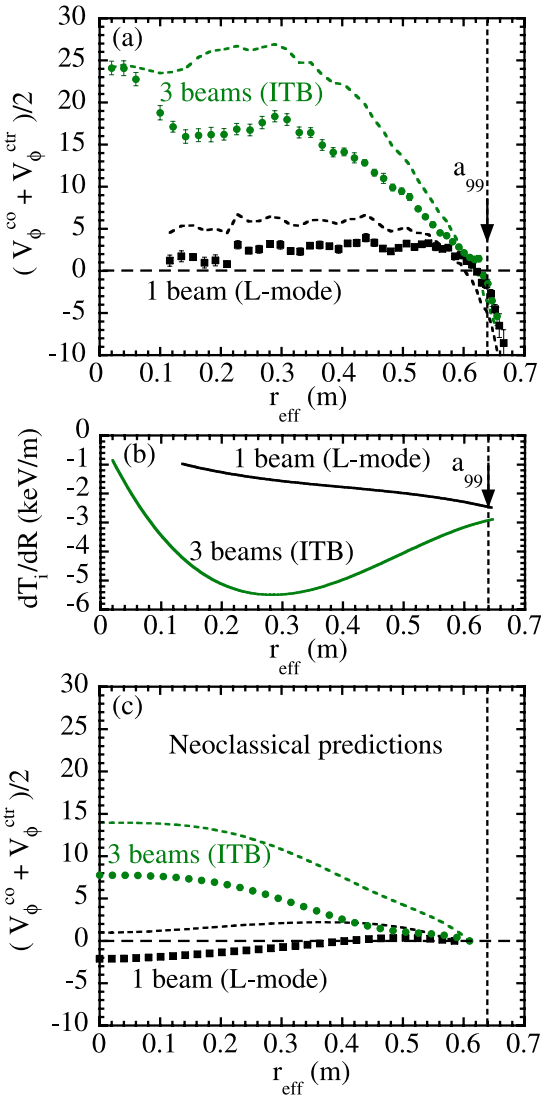

Figure 2. Radial profile of (*a*) the average of the toroidal rotation velocity of carbon measured (closed symbols) main ion (dashed line) and (*b*) ion temperature gradient and (*c*) neoclassical predictions (carbon: symbols and main ion: dashed lines) in plasmas with the co-NBI dominant discharge and plasmas with the counter-NBI dominant discharge plotted in figure 1, The plasmas with one NBI are in the L-mode, while those with three NBIs are in the ITB-mode.

rotation appears after the increase in the temperature gradient. The change in the toroidal rotation just after the onset of NBI is due to the NBI torque and the change in the toroidal rotation well after the NBI onset is due to the internal torque driven by the ion temperature gradient. Figure 3 shows the radial profiles of ion temperature, toroidal rotation velocity and the time derivatives of the toroidal rotation velocity at various time slices after the three NBs (1 co-injection and 2 counter-injection) are injected. After the onset of three beams, the ion temperature increases in the core region of $r_{\rm eff} < 0.45$ m and its profile becomes peaked at the plasma centre. The ion temperature in the L-mode region (outside of the ITB region) slightly decreases after the formation of the ITB. The increase in the ion temperature gradient is not as significant as that observed in the ITB plasmas in tokamaks, where the transport improvement is observed only in a narrow region in the plasma, not the entire plasma. The time behaviour of the toroidal rotation profiles is quite interesting as seen in figure 3(*b*). Plasmas rotate in the counter-direction which is the same direction of dominant beam torques near the plasma centre. However, plasmas rotate in the co-direction at the half of the plasma minor radius where the ion temperature gradient is large. The peak of the co-rotation has the same order of magnitude as the counter-rotation at the plasma centre. The difference in the time response of these counter-rotations at the plasma axis and co-rotation at the off-axis can be clearly seen in the radial profile of the time derivatives of toroidal rotation velocity as seen in figure 3(*c*). In the early phase of $t = 2.09$ s, the change in the toroidal rotation velocity is in the counter-direction and localized near the plasma centre of $r_{\rm eff} < 0.3$ m while the change in the toroidal rotation velocity in the later phase of $t = 2.29$ s is in the co-direction and peaked off the axis of $r_{\rm eff} \sim 0.3$ m. The radial profiles of the time derivative of the toroidal rotation velocity represent the radial profile of external toroidal torque due to the external torque driven by the NBI and the internal torque driven by the ion temperature gradient and curvature, respectively. The time scale of the change in the spontaneous rotation is 0.2 s, which is comparable to the time scale of the ion temperature profile change, while the change in the spontaneous rotation has a significant delay of 0.2 s, which is longer than the global energy confinement time of ∼0.04 s.

It should be noted that the radial profiles of toroidal rotation in the counter-NBI dominant discharge, where the sign of the toroidal rotation flips at $r_{\rm eff} = 0.15$ m, cannot be explained by momentum pinch. If there is a momentum pinch (inward transfer of momentum) in the plasma, the inward transfer of negative momentum (outward transfer of positive momentum) should exist for $r_{\rm eff} < 0.15$ m and the inward transfer of positive momentum should exist for $r_{\rm eff} > 0.15$ m. Then the artificial source of positive momentum, which breaks the conservation of angular momentum, is necessary at the rotation zero cross point of $r_{\rm eff} = 0.15$ m. Therefore, the peaked co- or counter-toroidal rotation might be explained by the momentum pinch, but the bi-directional toroidal rotation profile observed in LHD, which has both positive and negative sign (rotation in co- and counter-directions), can never be explained by the concept of momentum pinch.

3. Relation between the velocity gradient and ion temperature gradient and curvature

By including the non-diffusive term of momentum flux as an off-diagonal term between momentum and heat fluxes, the radial flux P_ϕ of the momentum transport can be written as

$$P_\phi(r) = \frac{1}{r}\int_0^r r'\left(T(r') - \frac{{\rm d}[m_{\rm i}n_{\rm i}(r')V_\phi(r')]}{{\rm d}t} - \mu_\parallel m_{\rm i}n_{\rm i}(r')V_\phi(r')\right){\rm d}r', \quad (1)$$

$$\frac{P_\phi}{m_{\rm i}n_{\rm i}} = -\left[\mu^D\nabla V_\phi - \left(\mu_1^N + \mu_2^N\alpha\right)v_{\rm th}\frac{\nabla T_{\rm i}}{T_{\rm i}}\right], \quad (2)$$

$$\alpha = a^2\frac{\nabla^2 T_{\rm i}}{T_{\rm i}}, \quad (3)$$

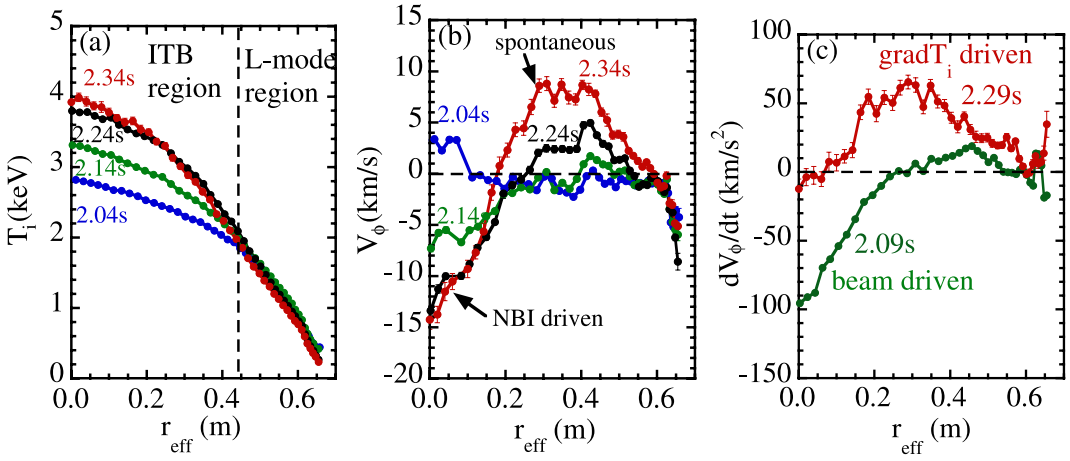

Figure 3. Radial profiles of (*a*) ion temperature, (*b*) toroidal rotation velocity, (*c*) time derivative of toroidal rotation velocity at various time slices after the turn on of the three NBIs.

where T, m_i, n_i, V_ϕ, v_th, a, $\mu_\parallel$ are the external toroidal torque density, ion mass, ion density and toroidal rotation velocity, ion thermal velocity and minor radius and parallel viscosity in the toroidal direction, respectively. The damping of toroidal rotation due to the parallel viscosity can be important near the plasma edge or in the configuration where the helical ripple is large [30]. However, this term can be neglected near the plasma core, because the parallel viscosity drops sharply towards the plasma centre [31] and the toroidal rotation damping due to the parallel viscosity is much smaller than the damping due to the anomalous perpendicular viscosity similar to the momentum transport in tokamaks.

The μ^D and μ_1^N are the coefficients of diffusive terms and non-diffusive terms proportional to the first derivative of the ion temperatures (T_i gradient). The μ_2^N and α are the coefficient of the curvature correction term and the normalized second derivative of the ion temperatures (T_i curvature). In this equation, the internal torque is expressed as a non-diffusive term of the momentum flux and only external torque is treated as a momentum source with $P_\phi(r)$. In principle, the non-diffusive term in this equation can be replaced as the internal torque expressed as $(1/r)\nabla[m_\mathrm{i}n_\mathrm{i}r(\mu_1^\mathrm{N} + \mu_2^\mathrm{N}\alpha)v_\mathrm{th}\nabla T_\mathrm{i}/T_\mathrm{i}]$. In general, the mechanism to determine the magnitude of the non-diffusive term is complicated and cannot be expressed with a simple formula. Here, the first derivative and the second derivative of the ion temperature radial profile (temperature gradient and curvature) are taken as non-diffusive terms, for simplicity. At the zero radial flux (for example in the case of experiment with no external torques), if $\mu_1^\mathrm{N} \propto \mu^\mathrm{D}$ and $\mu_2^\mathrm{N} \propto \mu^\mathrm{D}$, the gradient term of the radial flux of momentum transport contributes to the spontaneous rotation proportional to T_i, while the curvature term of the radial flux contributes to the spontaneous rotation proportional to $\partial T_\mathrm{i}/\partial r$.

Figure 4 shows the contour plot of ion temperature gradients and toroidal rotation velocity gradients in plasmas with the counter-NBI dominant discharge and in plasmas with the co-NBI dominant discharge. As seen in figure 4(*a*), the ITB region appears at $r_\mathrm{eff}/a_{99} = 0.7$ and $t = 2.15$ s as indicated with an abrupt increase in the ion temperature gradient. After the formation of the ITB, the ion temperature gradient exceeds 5 keV m^{-1} and the ITB region, where the ion temperature gradient is large, expands towards the plasma centre. The positive velocity gradient ($-\partial V/\partial r < 0$) appears near the plasma centre in the plasmas with the counter-NBI dominant discharge, while the negative velocity gradient ($-\partial V/\partial r > 0$) is observed near the plasma centre. These gradients are due to the external NBI torque. The negative gradients observed at $r_\mathrm{eff}/a_{99} = 0.7$ both in the co- and counter-NBI discharges are due to the non-diffusive term of momentum flux as seen in figures 4(*b*) and (*d*). As discussed before, the increase in the velocity gradient for the spontaneous rotation appears 0.1 s after the increase in the velocity gradient by the external NBI torque.

In order to investigate the existence of temperature curvature terms in the momentum flux, the radial profiles of the ion temperature curvature (the second derivative of the ion temperature) are plotted in figure 5. The average of the velocity shear is derived from the velocity gradient in plasmas with the co-dominant discharge and counter-dominant discharge to evaluate the contribution of the spontaneous rotation. Since the perpendicular viscosity, μ_D, is non-linear, the average of toroidal rotation velocity shear of the two plasmas with co-NBI dominant and counter-NBI dominant discharge is not identical to the velocity shear due to the spontaneous rotation in the plasma without net toroidal torque. However, the average of the toroidal rotation velocity shear is taken to test the existence of an ion temperature curvature driven term (the third term of equation (2)), for simplicity. The average of velocity shears has two peaks; one is located at $r_\mathrm{eff}/a_{99} = 0.8$ and the other is located at $r_\mathrm{eff}/a_{99} = 0.1$. The peak near the plasma edge corresponds to the region where the ion temperature curvature is positive and large. This peak suggests that there is an ion temperature curvature term in the momentum flux. The peak near the plasma axis is due to the imbalance of the beam deposition, where the beam deposition of co-NBI is more peaked than the beam deposition of counter-NBI because of the difference in the orbits of fast ions. The velocity shear of the toroidal rotation and the temperature gradient is strongly coupled. When the $E \times B$ shear due to the toroidal rotation is large enough, it is expected that the turbulence suppression due to the $E \times B$ contributes to the increase in the temperature gradient through the reduction in

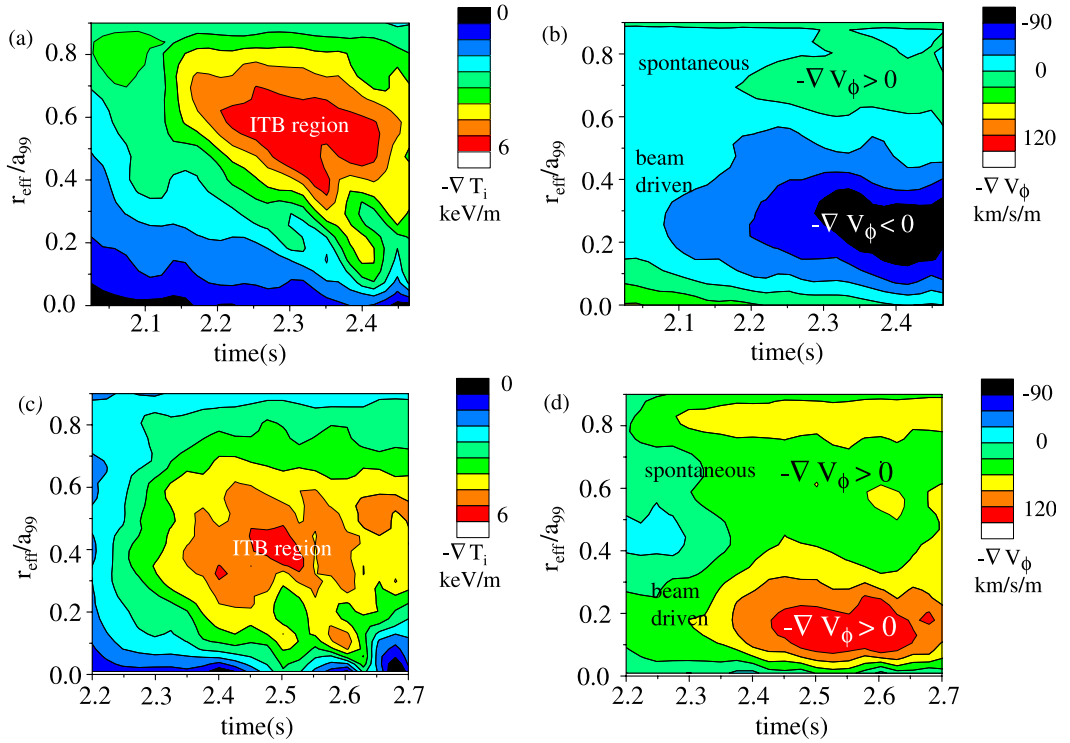

Figure 4. Contour plot of (*a*) ion temperature gradient and (*b*) toroidal rotation velocity gradient in the plasmas with counter-NBI dominant discharges and (*c*)(*d*) those in the plasmas with co-NBI dominant discharges.

thermal diffusivity. There is another important mechanism driving the spontaneous toroidal rotation due to the temperature or pressure gradient [10, 23]. Because of this process, the increase in the temperature gradient affects the toroidal rotation and its shear. Therefore, it is important to investigate the causality between the temperature gradient and the velocity shear by plotting a Lissajous figure.

Figure 6 shows the relation between the ion temperature gradient and the velocity shear of the toroidal rotation during the formation of an ITB in the plasmas with the counter-NBI dominant discharge. Near the plasma centre of $r_{\rm eff}/a_{99} = 0.25$, the relation between the temperature gradient and velocity shear is linear; which is due to the heating and momentum injection in the counter (negative) direction. However, there is a clear distortion from the linear relation observed at half of the plasma minor radius ($r_{\rm eff}/a_{99} = 0.37$ and 0.47). The velocity shear increases in the co-direction after the increase in the ion temperature gradient with a delay time on the order of the momentum confinement time. The increases in the velocity shear take place when the ion temperature gradient reaches a certain level, which indicates that the process driving the spontaneous rotation is non-linear, which is consistent with the fact that the relation between the spontaneous rotation and the temperature gradient is also non-linear.

In the discharges with carbon pellet injection, the density profile is peaked just after the pellet injection and it becomes flat as the electron density decreases afterwards. During the decay phase of density, the ion temperature profile becomes peaked. Therefore, the ion pressure gradient is more or less constant in time, while the ion temperature gradient and velocity shear increase ($t < 2.27$ s) as seen in figure 7. The

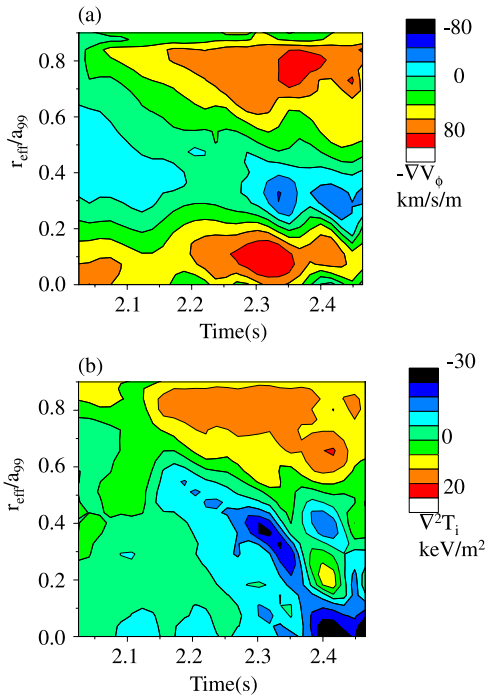

Figure 5. Contour plot of (*a*) the average of the toroidal rotation velocity shear and (*b*) the average of the second derivative of the ion temperature of the two plasmas in co-NBI dominant and counter-NBI dominant discharges.

spontaneous rotation appears after the increase in the ion temperature gradient ($2.27\,s < t < 2.43$ s) and velocity shear keeps increasing even in the steady state of the ion temperature gradient. Please note that the ion pressure gradient decreases

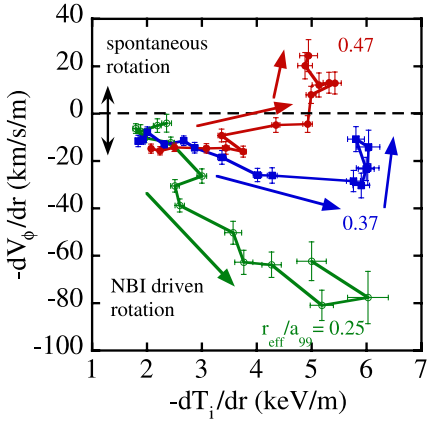

Figure 6. Relation between the ion temperature gradient and the toroidal rotation velocity gradient in plasmas with the counter-NBI dominant discharges.

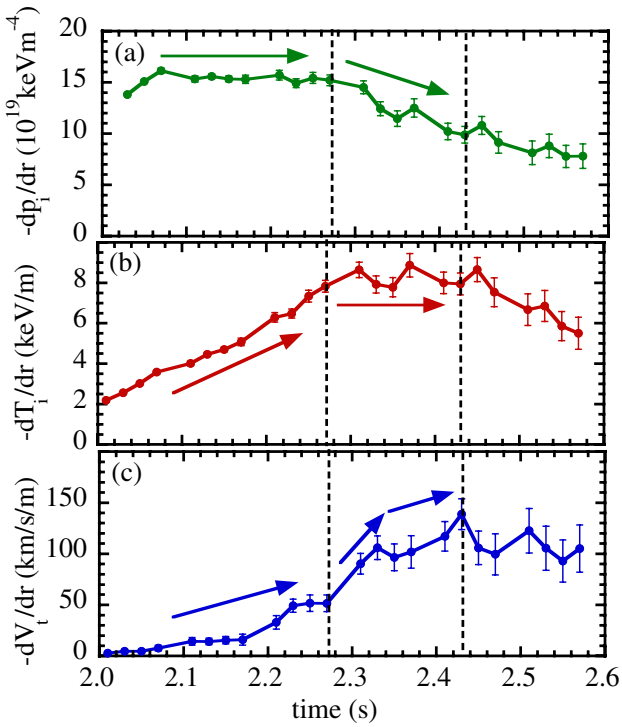

Figure 7. Time evolution of (*a*) ion pressure gradient, (*b*) ion temperature gradient and (*c*) velocity shear in the co-NBI dominant discharge with carbon pellet injection.

while the velocity shear increases. This observation suggests that the ion temperature gradient rather than the ion pressure gradient is the driving force of spontaneous rotation velocity, which is in contrast to the spontaneous rotation observed in JT-60U [17].

It is interesting to study the hysteresis in the relation between the velocity and the temperature gradient because the mechanism driving the spontaneous rotation has non-linear characteristics. A clear hysteresis is observed in the stronger ITB, where the ion temperature gradient reaches 9 keV m^{-1} as seen in figure 8. Please note that this is the discharge with the co-NBI dominant and the velocity shear near the plasma centre increases in the direction of co-NBI. Although the ion

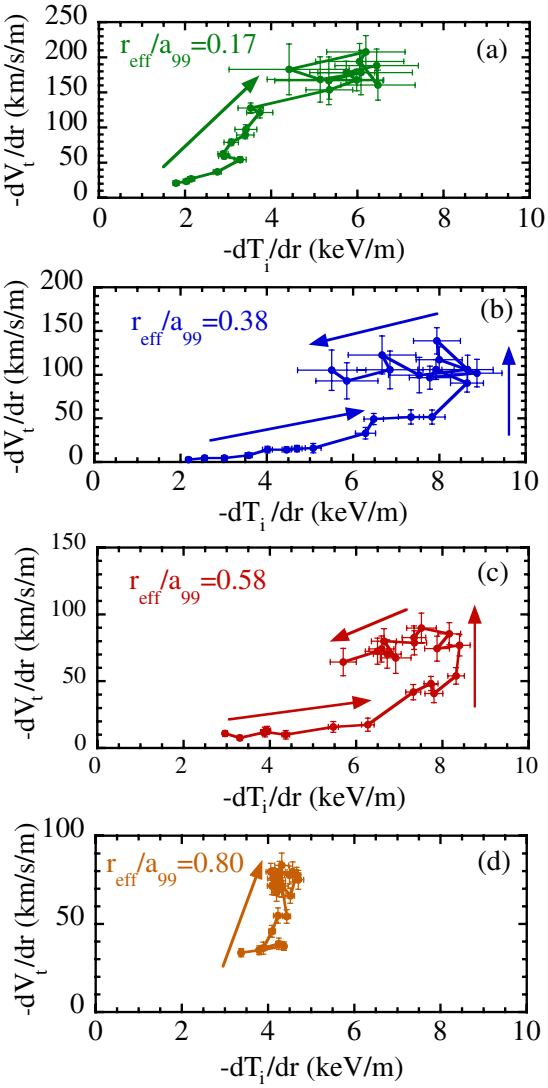

Figure 8. The hysteresis curve in the relation between the ion temperature gradient and toroidal rotation velocity gradient in the plasmas with the co-NBI dominant discharges.

temperature gradient starts to decrease in the later phase of the ITB period, the velocity gradient maintains a large value at $r_{\rm eff}/a_{99} = 0.35, 0.85$. This observation indicates that the spontaneous rotation is a transitional phenomenon and there are two modes in the spontaneous rotation; one is a small spontaneous rotation and the other is a large spontaneous rotation. The control parameter for this transition seems to be a temperature gradient. It is interesting that the non-diffusive term as well as the diffusive term of the momentum transport ($\mu_1^{\rm N}$ and $\mu_2^{\rm N}$ as well as $\mu^{\rm D}$) can be bifurcate, while only the diffusive term ($\chi_{\rm i}$) can be bifurcate in the heat transport.

The deposition of beam energy and the beam torque to ions becomes significant only after the beam energy decreases to the critical energy of $\sim 15 T_{\rm e}$ ($T_{\rm e}$ is electron temperature), where the beam energy deposition to ions is equal to that to electrons. Therefore, the ion heating is delayed with respect to the electron heating by $\sim$0.15 s. However, after the beam energy drops to the critical energy, the slowing down time of the beam energy and the velocity becomes $\sim$0.03 s and

$\sim$0.06 s, respectively. Therefore, the time constants for the heating and torque are dominated by the slowing down time of the beam to the critical energy and smaller than the time constant of the evolutions of temperature and velocity. When there is no spontaneous rotation in the plasma such as seen in figure 1(*a*), the time scales of change in ion temperature and plasma rotation are similar ($\sim$0.2 s). Since both time scales are similar, the relation between the ion temperature gradient and the velocity shear near the plasma centre ($r_{\rm eff}/a_{99} = 0.25$ in figure 6 and $r_{\rm eff}/a_{99} = 0.17$ in figure 8) is linear. It should be noted that while the beam driven rotation depends on the direction of the NBI; $-{\rm d}V_\phi/{\rm d}t < 0$ for counter-NBI (figure 6) and $-{\rm d}V_\phi/{\rm d}t > 0$ for co-NBI (figure 8), the spontaneous rotation is always positive ($-{\rm d}V_\phi/{\rm d}t > 0$) regardless of the direction of the NBI.

4. Discussion

The detailed analysis of the velocity shear of the spontaneous rotation shows interesting characteristics of the spontaneous rotation. This is the case that the increase in the velocity gradient is the result of an increase in the ion temperature gradient and not the cause. In general, the velocity shear due to the temperature gradient would contribute to the formation of an ITB as a feedback process, when the direction of the spontaneous rotation is the same as the direction of increasing $E_r \times B$ shear. The experimental data clearly show that the driving mechanism of the spontaneous rotation is non-linear, which results in the hysteresis between the temperature and velocity gradients. It is well known that there are two states in the heat transport; one is L-mode and the other an improved mode such as H-mode or ITB. In momentum transport, there are also two states; one is a small spontaneous rotation state and the other is a large spontaneous rotation state. The transition from small to large spontaneous rotation is triggered by the increase in the temperature gradient in LHD. The transition phenomenon is also observed in the rotation flip in the TCV tokamak [15].

It is difficult to distinguish the temperature gradient term from the temperature curvature term in the momentum flux, because the gradient and curvature are strongly coupled. However, the temperature gradient term (which results in $V_\phi^{\rm spon}(r) \propto T_{\rm i}(r)$) was observed in the L-mode discharge [10, 15], while the temperature curvature term (which results in $V_\phi^{\rm spon}(r) \propto \partial T_{\rm i}(r)/\partial r$) has been often observed in the plasma with an ITB [12]. This would be due to the fact that there is almost no curvature or at least small curvature in the L-mode plasma, while the temperature curvature tends to increase significantly in plasmas with an ITB. Although there are two off-diagonal terms, one proportional to the temperature gradient and the other proportional to the temperature curvature, this does not mean that there are two physics mechanisms for driving spontaneous rotations. The most possible candidate of the physics mechanism for the first and second derivative is the residual stress [34] which is driven by the turbulence, and the turbulence in the plasmas depends on the temperature gradient and curvature. Therefore, the gradient and curvature terms are just the first and second order expansions of the temperature dependence on turbulence.

Acknowledgments

The authors would like to thank the technical staff in LHD for their support of these experiments. This work is partly supported by a Grant-in-aid for Scientific research (18206094) of MEXT Japan. This work is also partly supported by the National Institute for Fusion Science grant administrative budget, NIFS05LUBB510.

References

[1] Suchewer S. *et al* 1981 *Nucl. Fusion* **21** 1301
[2] Brau K. *et al* 1983 *Nucl. Fusion* **23** 1643
[3] Rice J.E. *et al* 1997 *Nucl. Fusion* **37** 421
[4] Ida K. *et al* 1991 *Nucl. Fusion* **31** 943
[5] Eriksson L.-G. *et al* 1992 *Plasma Phys. Control. Fusion* **34** 863
[6] Rice J. *et al* 1998 *Nucl. Fusion* **38** 75
[7] Ida K. *et al* 2001 *Phys. Rev. Lett.* **86** 3040
[8] deGrassie J.S. *et al* 2004 *Phys. Plasmas* **11** 4323
[9] Nagashima K. *et al* 1994 *Nucl. Fusion* **34** 449
[10] Ida K. *et al* 1995 *Phys. Rev. Lett.* **74** 1990
[11] Koide Y. *et al* 1994 *Phys. Rev. Lett.* **72** 3662
[12] Sakamoto Y. *et al* 2001 *Nucl. Fusion* **41** 865
[13] Ernst D.R. *et al* 1998 *Phys. Plasmas* **5** 665
[14] Rice J.E. *et al* 2001 *Nucl. Fusion* **41** 277
[15] Bortolon A. *et al* 2006 *Phys. Rev. Lett.* **97** 235003
[16] Ida K. *et al* 1998 *J. Phys. Soc. Japan.* **67** 4089
[17] Yoshida M. *et al* 2008 *Phys. Rev. Lett.* **100** 105002
[18] Yoshinuma M. *et al* 2009 *Nucl. Fusion* **49** 075036
[19] Peeters A.G. *et al* 2006 *Plasma Phys. Control. Fusion* **48** B413
[20] Camenen Y. *et al* 2009 *Phys. Rev. Lett.* **102** 125001
[21] Dominguez R.R. *et al* 1993 *Phys. Fluids* B **5** 3876
[22] Gurcan O.D. *et al* 2007 *Phys. Plasmas* **14** 042306
[23] Yoshida M. *et al* 2006 *Plasma Phys. Control. Fusion* **48** 1673
[24] Ida K. *et al* 2009 *Nucl. Fusion* **49** 095024
[25] Hahm T.S. *et al* 2007 *Phys. Plasmas* **14** 072302
[26] Peeters A.G. *et al* 2007 *Phys. Rev. Lett.* **98** 265003
[27] Grucan O.D. *et al* 2008 *Phys. Rev. Lett.* **100** 135001
[28] Ida K. *et al* 2000 *Rev. Sci. Instrum.* **71** 2360
[29] Nakajima N. and Okamoto M. 1991 *J. Phys. Soc. Japan.* **60** 4146
[30] Ida K. *et al* 1991 *Phys. Rev. Lett.* **67** 58
[31] Ida K. and Nakajima N. 1997 *Phys. Plasmas* **4** 310
[32] Murakami S. *et al* 1995 *Trans. Fusion Technol.* **27** 256
[33] deGrassie J. *et al* 2007 *Phys. Plasmas* **14** 056115
[34] Diamond P.H. *et al* 2009 *Nucl. Fusion* **49** 045002